

Article

Assessment of Offshore Wave Energy Potential in the Croatian Part of the Adriatic Sea and Comparison with Wind Energy Potential

Andrea Farkas, Nastia Degiuli * and Ivana Martić

Faculty of Mechanical Engineering and Naval Architecture, University of Zagreb, Ivana Lučića 5, 10000 Zagreb, Croatia; andrea.farkas@fsb.hr (A.F.); ivana.martic@fsb.hr (I.M.)

* Correspondence: nastia.degiuli@fsb.hr; Tel.: +385-1-6168-269

Received: 16 May 2019; Accepted: 15 June 2019; Published: 19 June 2019



Abstract: The European Union is a leading patron for the introduction of renewable energy, having set a target that renewable sources will represent at least 27% of total energy consumption by the year 2030. Presently, the most significant Croatian renewable resource is hydropower, which is presently at its peak and will not develop further because of limited hydro resources. Therefore, the share of electricity generation from onshore wind farms in Croatia during in recent years has grown significantly. However, as the Croatian government has already made most of the concessions for possible locations of wind farms, the aim of the present study is to evaluate a different renewable energy resource, wave energy. An assessment of the offshore wave energy potential in the Croatian part of the Adriatic Sea is performed using data taken from WorldWaves atlas (WWA). WWA is based on satellite measurements, validated against buoy measurements and reanalysed by numerical wave modelling. This assessment was done for seven locations, and mean yearly energy is calculated for two offshore wave energy converters. Capacity factors were calculated for annual as well as for seasonal levels, and it was concluded that the bulk of the energy would be generated in autumn and winter. The most probable extreme significant wave height was determined at the investigated locations as well. Furthermore, the offshore wind energy potential was evaluated and compared to the wave energy potential.

Keywords: offshore wave energy; Adriatic Sea; WEC; extreme value analysis; seasonal variability; power matrix; capacity factor

1. Introduction

A significant increase in Greenhouse Gas (GHG) emissions occurred at the beginning of the Industrial Revolution; this is caused by human activities. Various destructive changes to the environment were noticed which are caused directly by GHG emission increases. Nowadays, when the atmospheric concentration of carbon dioxide has already exceeded the limit of 400 ppm, and since the demand for energy increases, the urgency for sustainable energy sources is even more highlighted. Most GHG emissions occur because of the combustion of carbon-based fuels, and therefore, the search for clean energy is continuously growing. A tremendous and essentially infinite energy source can be found in the world's seas, particularly in waves, temperature and salinity differences, and in tidal streams. Marine energy could play an important role in the generation of electricity in the long term, based on current demand levels, providing around 15-20% of electrical energy [1]. Recently, the most promising marine energy source is wave energy, because of easy predictability and availability around the world [2]. The future of wave energy harvesting relies upon further technological advancements of Wave Energy Converters (WEC), national policies and the number of large companies involved in this

industry [3]. An important issue regarding the development of wave harvesting is resource mapping at the national level [4]. Therefore, the assessment of wave energy resources, including temporal and spatial variability, is crucial for the selection of potential locations of wave farms [5,6], and can be divided into the characterisation of offshore and nearshore wave energy potentials [7]. A substantial amount of research has been carried out in order to assess the wave energy potential in various places. National wave energy resources were estimated for Australia [8] and Peru [9] at different depths. The annual wave energy resource for Australia varies from 1796 to 2730 TWh, while for Peru from 259 to 341 TWh, depending on the depth. In the case of Peru, the annual wave energy resource is about two times lower than the annual wind energy resource, and more than ten times higher than geothermal energy resource. Aboobacker [10] has estimated the wave energy resource of the Bay of Bengal at 19 locations; the highest obtained mean wave power was determined to be approximately 15 kW/m. A techno-economic analysis of the wave energy potential in the Philippines was performed in [11]. The authors determined a mean annual wave power in the range from 10 to 20 kW/m depending on the location. Lucero et al. [12] have assessed the nearshore wave energy potential along the central coast of Chile. The authors found that the median wave power ranges from 27 to 38 kW/m with high seasonal dependency. Contestabile et al. [13] have investigated the wave energy potential along the southern coast of Brazil. The authors estimated average wave power ranges from 8 kW/m to 14.5 kW/m at 20 m water depth. Furthermore, the authors recommended multifunctional structures, which would have both protection breakwater as well as wave harvesting capabilities. Sierra et al. [14] evaluated the wave energy potential along the western coast of Morocco. The authors found that mean wave power there varies from 7.83 to 29.94 kW/m, and that the annual energy varies from 6.90 to 15.64 GWh for Wave Dragon WEC and from 0.45 to 0.97 GWh for Pelamis WEC. The wave energy potential for Cape Verde is assessed in [15]. The obtained wave power is greater than 7 kW/m, but it depends strongly on the season, i.e., wave power in the summer is half the amount than in winter.

There is also a significant number of studies on the assessment of wave energy in areas with lower wave energy densities. Areas with wave powers lower than 2 kW/m are, for example: the Red Sea, Caspian Sea, Weifang Sea and Persian Gulf [16–19]. Wang et al. [20] have assessed the wave energy potential in Bohai sea, obtaining a mean wave power of up to 3.5 kW/m. In addition, the wave power in the Mediterranean Sea is also lower in comparison with that of open oceanic regions; it was assessed that the gross theoretical wave power resource for the Mediterranean Sea was about 37 GW, which represents 0.1% of global gross theoretical wave power resources [21]. The wave climate was analysed in several areas of the Mediterranean Sea in [22]. In this study, the authors determined the most energetic areas as well as the areas where the highest extreme values are expected. Analysing 31 locations, mostly along the coast of the Mediterranean Sea, the authors found that mean wave power varied from 1.8 to 15.1 kW/m. Besio et al. [23] assessed the wave energy potential utilising numerical simulations over a 35-year period. The authors found that the most energetic area in the Mediterranean Sea is the area in between Sardinia, Corsica, the Balearic Islands and the Northern coast of Algeria, with mean wave power around 10 kW/m. Furthermore, the authors concluded that there is a significant variability of wave power according to the month. Similar studies are performed in [24,25], and even though the length of hindcasted periods within the performed studies are different, the results regarding the spatial distribution and local magnitudes of mean wave power are almost the same. Thus, the highest values of mean wave power are obtained in the same area as those obtained in [23]. The lowest values of the mean wave power were obtained in the Adriatic Sea, i.e., below 2 kW/m. Franzitta et al. [26] analysed the renewable energy potential of the Maltese islands, focusing on the wave energy. The authors showed a significant seasonal variability in mean wave power, with the highest wave power being present in the winter, and concluded that this seasonal variability could be compensated for when combined with seasonal variability in solar energy. Evaluation and characterisation of wave energy resources for the Libyan Sea are performed in [27]. Even though the calculated wave powers are lower than those in open oceanic regions, the low variations of wave height and wave energy periods yield better predictability. Furthermore, lower extreme values in

this region, when compared to those in open oceanic regions, lead to the reduction of installation and maintenance costs. A preliminary investigation of the wave energy potential around the Italian coast, i.e., the Adriatic, Ionian, Tyrrhenian and Ligurian Seas, is shown in [28]. The authors concluded that a location near Alghero could be suitable for further analysis of wave energy harvesting. Bozzi et al. [29] also performed a feasibility study of the energy harvesting in the Italian seas, and analysed the capacity factors of three WECs. The authors found that the investigated WECs would remain idle for the majority of the year, and concluded that these WECs were oversized. Therefore, the authors investigated smaller rated WECs at two locations and found that downscaled devices have significantly higher capacity factors. Downscaled devices could be beneficial for wave energy harvesting around Crete as well, since these would be adapted for lower energetic sea areas [30].

Within this study, the determination of the wave energy potential in the Croatian part of the Adriatic Sea is performed. A detail analysis of offshore wave energy potential is done for seven locations in the central and northern Adriatic. Since the same location can have significantly different power production capabilities if different WECs are applied [31,32], within this study, two WECs were tested—i.e., Pelamis and Aqua Buoy—which are both considered offshore devices. Furthermore, the most probable extreme significant wave height was determined at the investigated locations, which is of significance for the design loads of offshore structures [27]. A comparison of the wave and wind energy potential for these seven locations within the Adriatic Sea is provided. Thus, the benefits and concerns regarding these two renewable energy resources are presented and analysed.

2. Materials and Methods

2.1. Offshore Wave Energy Potential

The wave data used for the assessment of the wave energy potential is taken from the WorldWaves atlas (WWA), which is a high-resolution interactive wind and wave atlas. The WWA depends generally on satellite measurements, which were validated against buoy measurements and reanalysed by numerical wave modelling [33]. Satellite altimeter data at full resolution was obtained based from the Geosat, TOPEX, Topex/Poseidon, Jason, EnviSat, Geosat Follow-On, Jason-2 and Jason-1s satellites; this data covers the period from July 1992 to January 2016. Every time a satellite passes, wave height is measured about each 6 km along the tracks, while wind speed is approximated using a parametric model. The obtained data is validated against buoy measurements. In order to obtain adequately high temporal resolution and systematic and high-resolution data, measurements are combined with third-generation wave model WAM for deep sea waves. WAM is run every day by the European Centre for Medium-Range Weather Forecasts (ECMWF), and this numerical model is calibrated with satellite measurements. For the Adriatic Sea, the WWA database comprises a data for 39 uniformly distributed locations, as shown in Figure 1. For every location, ten wave parameters and two wind parameters are provided at six-hour intervals, i.e., four times per day; see Table A1 (in Appendix A). Thus, every location has a total of 34,460 data outputs. In this study, seven locations within the Croatian part of the Adriatic Sea were selected for assessments of offshore wave energy potential, as shown in Figure 1.

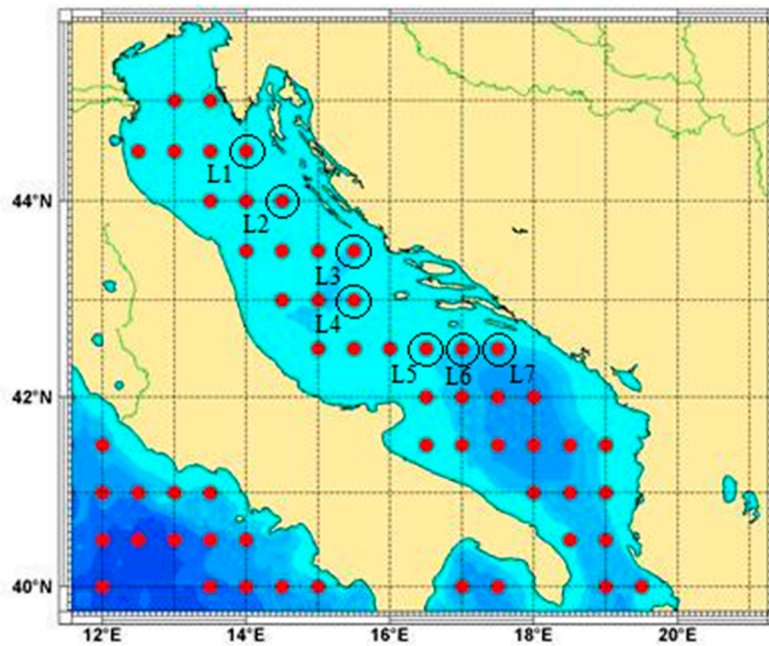


Figure 1. Offshore grid points provided in WWA for the Adriatic Sea. Source: Oceanor.

It should be noted that the mean wave period presented in Table A1 is the wave energy period defined as follows [2,13]:

$$T_E = \frac{m_{-1}}{m_0}, \quad (1)$$

where m_n is the n -th order spectral moment.

This represents the period of a sinusoidal wave which has the same energy as an actual sea-state. Significant wave height can be obtained as follows [2,13]:

$$H_S = 4 \sqrt{m_0}. \quad (2)$$

It should be noted that for some data outputs, there are occasional missing data, i.e., not all WWA wave and wind parameters are given; see Table 1. The missing data was randomly distributed and did not cause distortions to occur in the analysis, i.e., missing season, etc. It should be noted that data logs which have missing data were excluded prior to processing and analysing the wave statistics, as done in [34].

Table 1. Selected locations in the Adriatic Sea.

Location	Latitude	Longitude	Number of Data Outputs
L1	44.5° N	14.0° E	33,033
L2	44.0° N	14.5° E	33,364
L3	43.5° N	15.5° E	33,438
L4	43.0° N	15.5° E	34,021
L5	42.5° N	16.5° E	33,913
L6	42.5° N	17.0° E	33,857
L7	42.5° N	17.5° E	33,775

The offshore wave climate at any location consists of different wave fields, which include both swells and wind waves. The offshore wave power per unit of wave front length can be estimated directly from hindcast wave data as follows [2,13]:

$$P = \frac{\rho g^2}{64\pi} H_S^2 T_E, \quad (3)$$

where ρ is the sea water density and g is the gravitational acceleration.

Equation (3) is derived for deep water. Namely, the wave power per unit of wave front length is obtained as a product of the averaged energy density and the group velocity. The averaged energy density per unit horizontal area can be calculated as follows:

$$E = \frac{1}{16} \rho g H_S^2. \quad (4)$$

For deep water, the group velocity which represents an energy transport velocity is equal to

$$c_g = \frac{g T_E}{4\pi}. \quad (5)$$

In order to calculate the annual energy potential at certain locations, wave scatter diagrams should be generated. Wave scatter diagrams represent a matrix which divide all sea states into classes. Thus, all data outputs should be organised and divided into classes of H_S and T_E . Two wave scatter diagrams were made for each location. Both wave scatter diagrams have H_S classes with 0.5 m increments; the difference among these two diagrams is in T_E classes. Namely, one has T_E classes with 0.5 s increments and the other with 1 s increments. Thus, every class includes the number of occurrences of that sea state class over a period of 24 years. Furthermore, for each sea state, occurrence (p_{ij}) is calculated based on the number of the hours per year. It should be noted that each class represents a certain energy bin. As the energy output of certain WECs is dependent on the wave energy distribution among the sea states, estimations of annual electrical energy can be calculated as follows [31]:

$$P_E = \sum_{i=1}^{n_{T_E}} \sum_{j=1}^{n_{H_S}} p_{ij} P_{ij}, \quad (6)$$

where P_{ij} is the electric power for a certain energy bin. The values of P_{ij} are presented in the power matrices of certain WECs.

Within this study, two offshore WEC were considered: Pelamis and Aqua Buoy; see Figure 2. Considering the power matrices of different WECs, the authors concluded that Aqua buoy and Pelamis would be the most suitable locations to carry out investigations.



Figure 2. The two WECs considered in this study: Pelamis (Left) and Aqua Buoy (Right) [35].

Pelamis is an offshore device that has a length of 150 m and a tube diameter of 4.63 m; it consists of four tubular sections which move relative to each other. These sections are connected by three hinges which convert the motion of the tubular sections. The mooring system for Pelamis consists of a three-point slack mooring configuration which allows it to turn into the wave direction within its mooring constraints. The rated power of Pelamis is 750 kW. Aqua Buoy is an offshore device that has buoy diameter of 6 m and a length of 30 m. It is a free-floating, heaving point absorber, which reacts against a submersed reaction tube. The mooring system for Aqua Buoy consists of three slack mooring configurations. The rated power of Aqua Buoy is 250 kW [35]. The power matrices for the two WECs are shown in Tables A2 and A3 (Appendix A). The values in the first column and row therein are the mean values of certain classes.

Once the annual wave energy is obtained, i.e., P_E , the average electric power is calculated as follows:

$$P_{E,average} = \frac{P_E}{t}, \quad (7)$$

where t is the number of hours in one year, i.e., 8760 h.

WEC performance is usually defined through the capacity factor, which is defined as follows [36]:

$$C_f = \frac{P_{E,average}}{R_p} \times 100\%, \quad (8)$$

where R_p is the rated power of certain WECs.

Besides the determination of the wave energy potential at certain locations, another important examination should be performed, i.e., the calculation of extreme sea states [22]. Thus, the long-term performance of WECs is dependent on the occurrence of extreme sea states at a given location. Therefore, a structural reliability assessment should include the determination of the most probable extreme significant wave height which will occur at the location where the WEC is installed over a certain return period, i.e., during the lifetime of the WEC [37]. Within this paper, the 3-parameter Weibull probability density function (PDF) is used as a marginal PDF of H_S :

$$f_{H_S}(\hat{H}_S) = \frac{\alpha}{\theta} \left(\frac{\hat{H}_S - \varepsilon}{\theta} \right)^{\alpha-1} \exp \left\{ - \left(\frac{\hat{H}_S - \varepsilon}{\theta} \right)^\alpha \right\}, \quad (9)$$

where α is the shape, θ is the scale and ε is the location parameter. These parameters are obtained from the data outputs using the least squares method, as explained in [34,38].

Cumulative distribution function (CDF) for the 3-parameter Weibull PDF can be obtained as follows:

$$F(\hat{H}_S) = \int_0^{\hat{H}_S} f_{H_S}(\hat{H}_S) dH_S = 1 - e^{-\left[\frac{(\hat{H}_S - \varepsilon)}{\theta} \right]^\alpha}. \quad (10)$$

Once the 3-parameter Weibull PDF is fitted for a certain location, which is PDF for a random variable \hat{H}_S , the probability of exceeding certain H_S in a particular return period (RP) can be obtained as follows [34,38]:

$$Q(H_S^{RP}) = \frac{T_{REG}}{N} \frac{1}{RP}, \quad (11)$$

where T_{REG} is the duration of uninterrupted observation and N is the number of samples, i.e., the total sum of output data as given in the wave scatter diagrams.

The value of a certain significant wave height being exceeded in specific RP can be obtained as follows [34,38]:

$$H_S^{RP} = \theta \left(-\ln(Q(H_S^{RP})) \right)^{1/\alpha} + \varepsilon. \quad (12)$$

It should be noted that T_{REG} should be at least 20% of RP [27]. Since, T_{REG} for this study is 23.5 years, H_S^{RP} can be calculated for RP for up to 117.5 years.

2.2. Offshore Wind Energy Potential

Even though the primal goal of this study was to investigate the wave energy potential in the Adriatic Sea, offshore wind energy potential for seven selected locations was also assessed, in order to make comparison between the two renewable energy resources. The wind energy potential estimation is based on the computational atmosphere model ALADIN (Aire Limitée Adaptation Dynamique développement InterNational). ALADIN is used for the prediction of heavy precipitation, intensive convection and strong winds, but also for research purposes [39]. Within this paper, an average wind speed at 80 m height (v_{W80}) is estimated according to ALADIN [40] for a one-year period in a 2 km × 2 km square area, as done in [39]; see Figure 3. Within this study, a wind turbine, the HQ 2000/WT 93, with a diameter of 93.2 m, is used for the assessment of the wind potential [41].

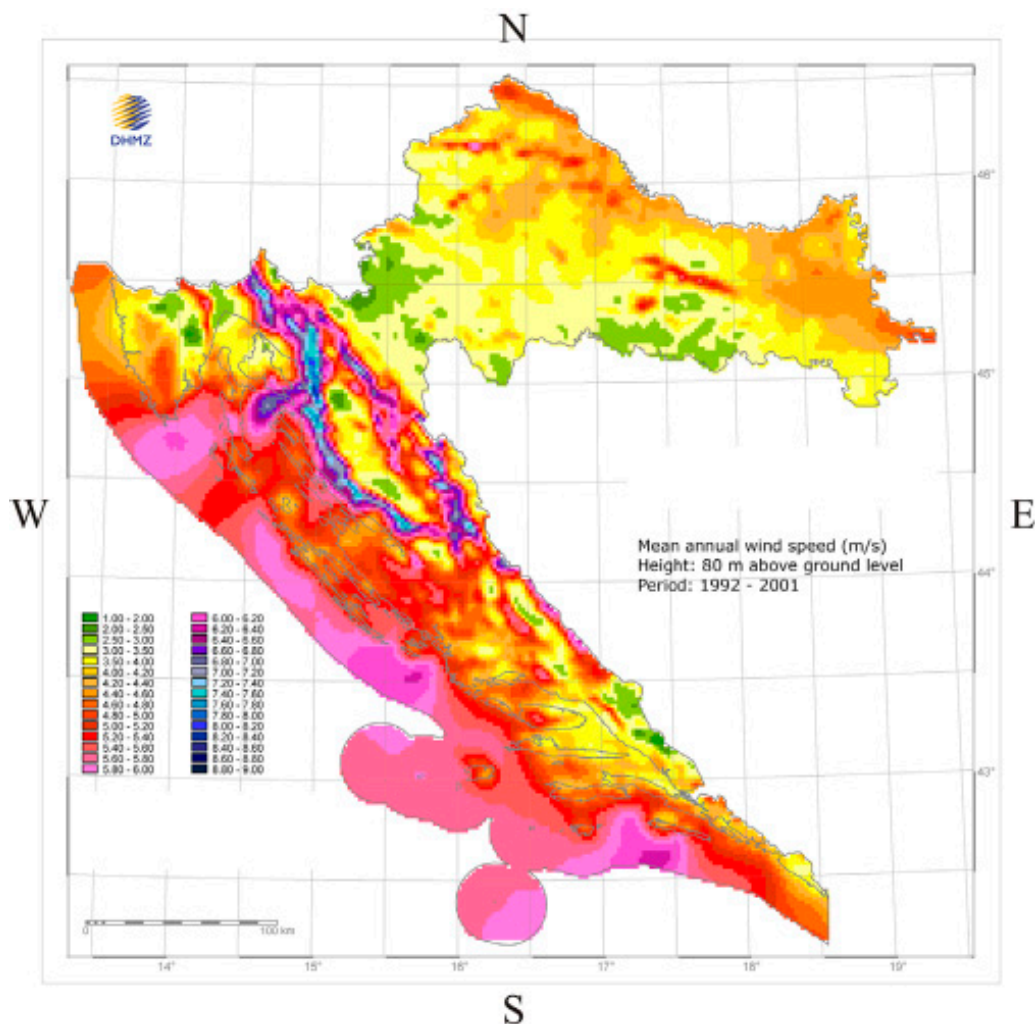


Figure 3. The average wind speed at 80 m height [40].

The average electrical power produced by one offshore wind turbine can then be determined as follows [39]:

$$P_{EW,average} = \frac{1}{2} C_P \rho_A v_{W80}^3 A, \quad (13)$$

where A is the area of wind turbine rotor, ρ_A is the air density and C_P is the power coefficient, i.e., 0.4.

Offshore wind turbines have some benefits over land wind turbines because of a nearly flat sea surface. Thus, almost constant average wind velocity at hub height is present, as well as weak

atmospheric turbulence. Therefore, these turbines have higher operating efficiencies and lower structural fatigue. It should be noted that the lower operating v_{W80} is 5 m/s [39].

3. Results and Discussion

3.1. Offshore Wave Energy Potential

Data outputs for the aforementioned locations in the Adriatic Sea are used for the creation of wave roses, wave power diagrams, and for the characterisation of the yearly energy. Also, a statistical analysis of the waves is performed. The obtained results, regarding mean values and standard deviations for both H_S and T_E , are shown in Table 2. The results are shown for annual and seasonal levels. The mean values of wave power are also shown.

Table 2. Wave climate parameters.

Location	L1					L2				
	Annual	Summer	Autumn	Winter	Spring	Annual	Summer	Autumn	Winter	Spring
$H_{S,mean}$, m	0.746	0.549	0.892	0.897	0.642	0.768	0.547	0.916	0.935	0.669
σ_{H_S} , m	0.575	0.375	0.654	0.664	0.461	0.595	0.363	0.684	0.68	0.494
$T_{E,mean}$, s	3.586	3.315	3.791	3.744	3.486	3.607	3.282	3.829	3.794	3.522
σ_{T_E} , s	0.932	0.844	1.017	1.009	0.900	0.978	0.822	1.041	1.009	0.922
P_{mean} , kW/m	1.959	0.818	2.821	2.859	1.303	2.133	0.798	3.105	3.126	1.486
Location	L3					L4				
	Annual	Summer	Autumn	Winter	Spring	Annual	Summer	Autumn	Winter	Spring
$H_{S,mean}$, m	0.764	0.550	0.892	0.925	0.689	0.809	0.581	0.937	1.000	0.725
σ_{H_S} , m	0.560	0.338	0.639	0.635	0.485	0.585	0.364	0.652	0.669	0.508
$T_{E,mean}$, s	3.647	3.291	3.870	3.861	3.567	4.182	3.687	4.473	4.531	4.053
σ_{T_E} , s	0.988	0.819	1.062	1.014	0.921	1.502	1.472	1.444	1.464	1.470
P_{mean} , kW/m	2.030	0.751	2.882	2.966	1.524	2.657	1.010	3.647	4.046	1.973
Location	L5					L6				
	Annual	Summer	Autumn	Winter	Spring	Annual	Summer	Autumn	Winter	Spring
$H_{S,mean}$, m	0.879	0.630	1.020	1.088	0.786	0.866	0.611	1.013	1.074	0.771
σ_{H_S} , m	0.611	0.354	0.689	0.704	0.515	0.623	0.345	0.713	0.724	0.516
$T_{E,mean}$, s	3.832	3.395	4.074	4.157	3.714	3.830	3.372	4.083	4.153	3.721
σ_{T_E} , s	1.023	0.774	1.087	1.076	0.941	1.046	0.775	1.117	1.099	0.968
P_{mean} , kW/m	2.782	1.007	3.851	4.320	1.994	2.784	0.937	3.936	4.351	1.951
Location	L7									
	Annual	Summer	Autumn	Winter	Spring					
$H_{S,mean}$, m	0.840	0.587	0.985	1.042	0.754					
σ_{H_S} , m	0.630	0.336	0.724	0.744	0.518					
$T_{E,mean}$, s	3.848	3.372	4.112	4.175	3.746					
σ_{T_E} , s	1.097	0.798	1.179	1.163	1.015					
P_{mean} , kW/m	2.685	0.862	3.891	4.333	1.913					

As shown in Table 2, the annual mean wave power for the seven analysed locations ranges from 1.959 kW/m to 2.784 kW/m. The highest annual value of P_{mean} was obtained for L6, located to the south-east of the island of Lastovo; almost the same annual value of P_{mean} was obtained at location L5, located to the south-west of the island of Lastovo. Furthermore, only a slightly lower annual P_{mean} was obtained at locations L4 and L7, located to the west of the island of Svetac and south of the island of Mljet. Locations L1 and L3, located to the west of the island of Susak and south-west of the island of Žirje had an annual value of P_{mean} near 2 kW/m, while location L2, located to the west of the island of Dugi otok had slightly higher annual P_{mean} . Mean annual values of H_S range from 0.746 m to 0.879 m, while standard deviations of H_S at the analysed locations ranged from 0.560 to 0.630 m. Mean annual values of T_E ranged from 3.586 to 4.182 s, while σ_{T_E} ranged from 0.932 to 1.502 s. It should be noted that the highest values of P_{mean} for all locations were obtained in the winter, with the highest P_{mean}

being obtained for L6, i.e., 4.351 kW/m. Slightly lower values of P_{mean} were noted in the autumn, while in the spring, the P_{mean} was more than half that in the winter for all locations. The lowest values of P_{mean} were obtained in the summer time, when P_{mean} values were mostly below 1 kW/m. For all the investigated locations, relatively high standard deviations were obtained compared to mean values. The predictability of the annual electrical energy, which can be determined from Equation (6), is not affected by higher values of standard deviations, as each sea state is divided into classes.

The monthly mean values of H_S , T_E and P were calculated for all locations. At locations L5 and L6 in January, February, March, November and December, P_{mean} was equal to or above 4 kW/m, while for L7, similar results were obtained, except for March, where slightly lower P_{mean} was obtained. Generally, during those months at all analysed locations, P_{mean} had a higher value than for other months. Only locations L5, L6 and L7 had P_{mean} values above 5 kW/m in December, with the highest P_{mean} being obtained at location L7, i.e., 5.068 kW/m. In Figure 4, the monthly mean values of H_S , T_E and P at location L6 are shown. It can be seen from this figure that H_S varies more than T_E , thus causing the variation of P .



Figure 4. The monthly mean value of H_S (top), T_E (middle) and P (bottom) for L6.

Furthermore, wave rose diagrams were made for all the investigated locations; see Figure 5. In order to make those diagrams, data outputs were sorted into classes of mean wave angles with $\Delta\vartheta = 10^\circ$. As shown in Figure 5, the bulk of wave power for most locations resulted from south-easterly (SE) waves, especially for L5, L6 and L7. However, for L1 and L2, the bulk of the wave power was provided by north-easterly (NE) waves. It should be noted that dominant winds which cause wind waves in the Adriatic Sea are “jugo” (SE) and “bura” (NE). These winds can reach storm conditions and induce extreme wave occurrences. At location L4, the bulk of the wave power was produced by northerly, south-easterly and southerly waves. Thus, it can be considered that this location has wave power which is supplied with the largest wave angle distribution. Significantly higher wave power is present at locations L5, L6 and L7 due to south-easterly waves, compared to the wave power present due to north-easterly waves at L1 and L2. Within this study, the bivariate distribution of wave energy production is investigated, i.e., the production of electrical energy depends solely on the significant wave height, energy period and certain sea state occurrences. However, for the implementation of WEC at certain locations, the direction and spreading of waves are very important factors as well. In other words, wave energy production depends on the directionality of the resource as well. Thus, depending on the wave direction, in order to enhance the electricity production, WEC should be directed optimally. Therefore, it would be beneficial to include operational characteristics which are able to optimise the production of the electrical energy [27].

Characterisation of mean yearly wave energy was obtained for seven locations in the Croatian part of the Adriatic Sea and for two offshore WECs; see Table 3 and Figures 6 and 7. Within Figures 6 and 7, the number inside each bin signifies the number of hours during one year of a certain sea state. The mean annual energy per meter is represented with the colour of each bin; furthermore, the lines shown in those figures represent wave power isolines.

Table 3. The mean yearly wave energy.

Location	Aqua Buoy		Pelamis	
	P_E , MWh	$P_{E,average}$, kW	P_E , MWh	$P_{E,average}$, kW
L1	14.945	1.706	104.204	11.895
L2	17.469	1.994	124.254	14.184
L3	20.387	2.327	122.143	13.943
L4	49.240	5.621	229.055	26.148
L5	35.417	4.043	194.336	22.184
L6	35.845	4.092	196.117	22.388
L7	37.623	4.295	197.536	22.550

Even though the highest mean wave power was obtained at location L6, the highest mean yearly wave energy for both Aqua Buoy and Pelamis was obtained at location L4. This can be attributed to a more favourable wave scatter diagram for L4 than for other locations. Obviously, at location L4, sea states which produce more electricity occur more often than at location L6; i.e., at L4, sea states with higher T_E occur more frequently, thus producing more electricity, as in higher T_E classes power output (P_{ij}) is higher. At L4, the mean yearly wave energy for Aqua Buoy was thus 49.24 MWh, and for Pelamis, 229.06 MWh. Locations L4, L5 and L6 have almost the same P_E for both WECs, while a significantly lower P_E was obtained at locations L1, L2 and L3. When compared to the $P_{E,average}$ obtained along the Portuguese nearshore [31], location L4 had around six times lower $P_{E,average}$ for Aqua Buoy and approximately four times lower for Pelamis, while the $P_{E,average}$ along the Atlantic coast of Morocco was approximately two to four times higher for Pelamis [14].

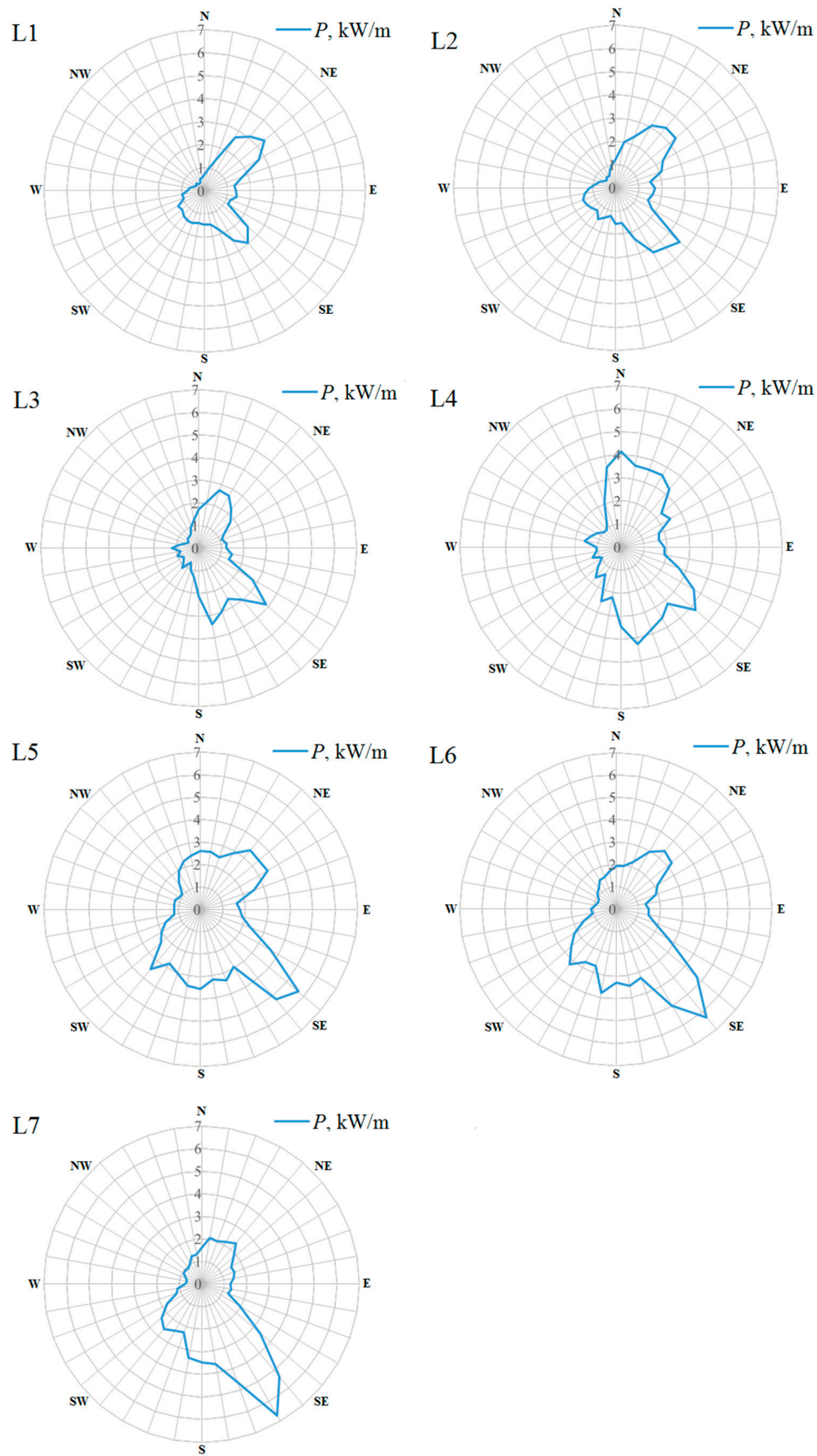


Figure 5. Wave roses for wave power at investigated locations.

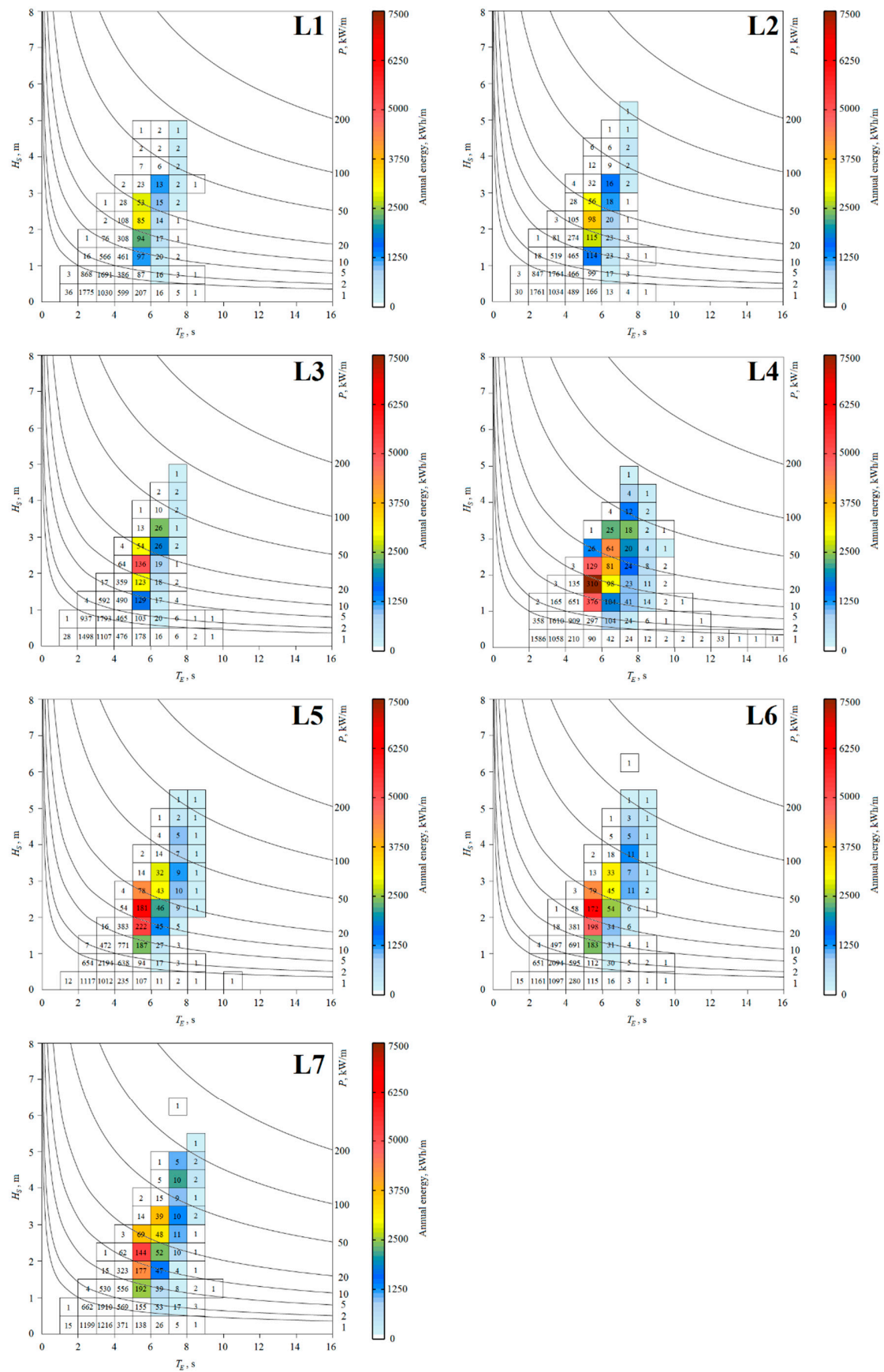


Figure 6. Characterisation of the annual wave energy at the investigated locations using the Aqua Buoy.

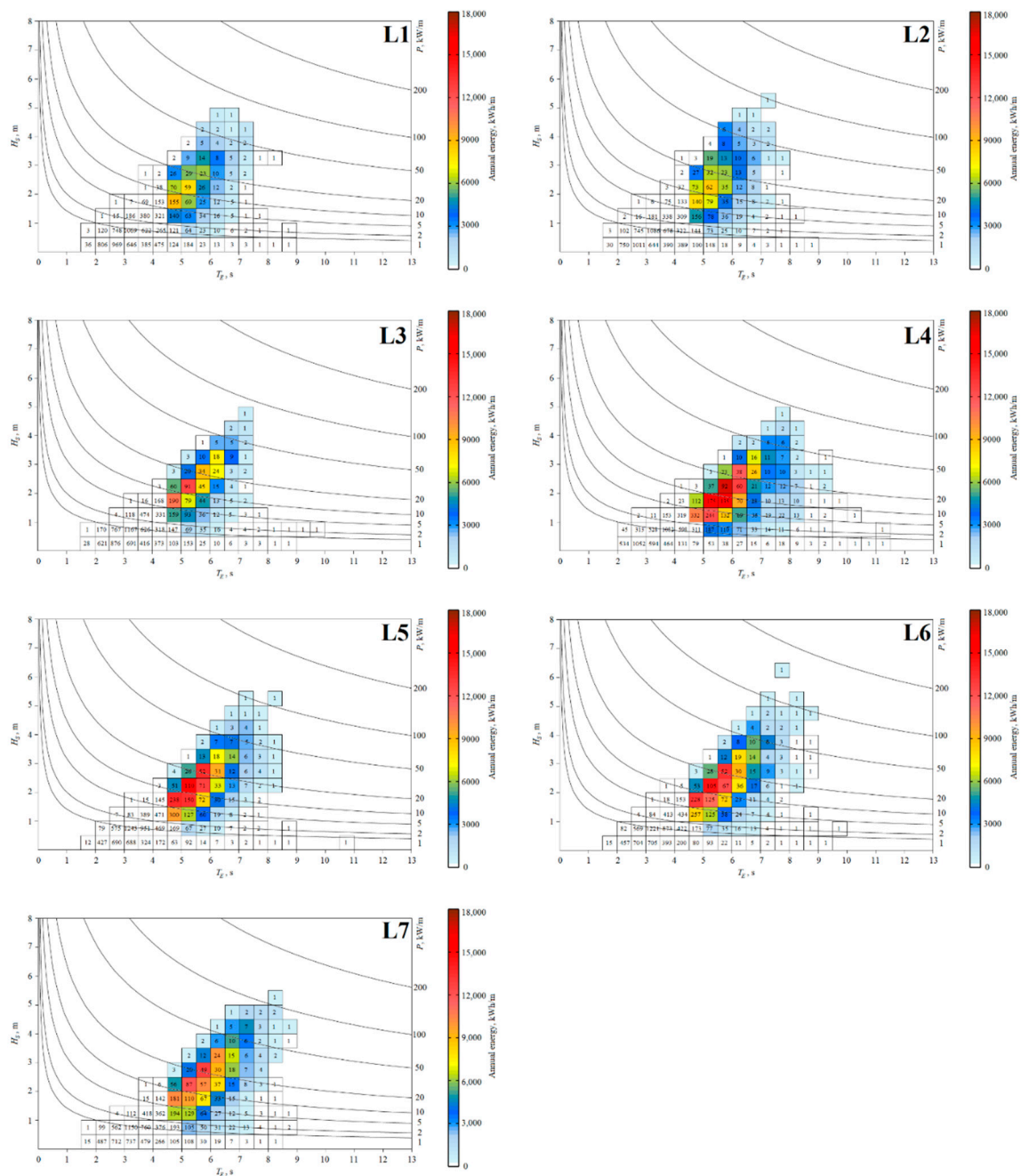


Figure 7. Characterisation of the annual wave energy at the investigated locations using the Pelamis.

As shown in Figure 6, the maximum energy for Aqua Buoy was concentrated in the bins with $H_S = 1.5\text{--}2\text{ m}$ and $T_E = 5\text{--}6\text{ s}$ at location L4, while for other locations this maximum was concentrated in the bins with $H_S = 2\text{--}2.5\text{ m}$ and $T_E = 5\text{--}6\text{ s}$. From Figure 7, it can be seen that the maximum energy for Pelamis was concentrated in the bin with $H_S = 2\text{--}2.5\text{ m}$ and $T_E = 5\text{--}5.5\text{ s}$ at locations L2–L6, in the bin with $H_S = 1.5\text{--}2\text{ m}$ and $T_E = 4.5\text{--}5\text{ s}$ for L1, in the bin with $H_S = 2\text{--}2.5\text{ m}$ and $T_E = 5.5\text{--}6\text{ s}$ for L4 and in the bin with $H_S = 2.5\text{--}3\text{ m}$ and $T_E = 5.5\text{--}6\text{ s}$ for L7.

Capacity factors were calculated for annual and seasonal levels, as shown in Table 4. This parameter takes into account the fraction of time in which WEC operates at full capacity. As shown in Table 4, low C_f were obtained for both WECs. Higher C_f were obtained for Pelamis, thus showing that it would be more suitable for the wave climate present in the Croatian part of the Adriatic Sea. The higher C_f obtained for Pelamis can be attributed to its power matrix, i.e., Pelamis can produce electrical

energy for lower T_E , which is present in the Croatian part of the Adriatic Sea. The highest annual C_f was obtained for Pelamis at L4: 3.49%. From Table 4, it can be seen that significant seasonal variability occurs at each investigated location. Thus, in the summer, the C_f of Aqua buoy was below 0.5%, while that of Pelamis was below 0.8%. On the other hand, for the autumn/winter, the C_f of Aqua buoy was below 3.81% and that of Pelamis was below 5.73%. It can be concluded that the bulk of the energy would be generated in the autumn and winter.

Table 4. Capacity factors.

WEC	C_f , %									
	Aqua Buoy					Pelamis				
Location	Annual	Summer	Autumn	Winter	Spring	Annual	Summer	Autumn	Winter	Spring
L1	0.68	0.10	1.16	1.02	0.43	1.59	0.27	2.59	2.58	0.86
L2	0.80	0.13	1.32	1.23	0.51	1.89	0.29	3.09	3.04	1.11
L3	0.93	0.08	1.58	1.48	0.58	1.86	0.21	3.02	3.04	1.17
L4	2.25	0.41	3.37	3.81	1.46	3.49	0.79	5.10	5.73	2.40
L5	1.62	0.19	2.52	2.87	0.93	2.96	0.45	4.49	5.14	1.81
L6	1.64	0.18	2.54	2.93	0.93	2.99	0.38	4.65	5.18	1.78
L7	1.72	0.17	2.66	3.09	0.98	3.01	0.36	4.70	5.20	1.82

Beside the assessment of wave energy potential in the Croatian part of the Adriatic Sea, an extreme value analysis was performed for the following return periods: 1, 5, 10, 20, 50 and 100 years. Therefore, the 3-parameter Weibull PDF was derived for each investigated location in order to represent PDF for H_S . The obtained Weibull parameters are shown in Table 5 for each location.

Table 5. Weibull parameters.

Location	α	θ	ε
L1	0.926	0.464	0.534
L2	0.935	0.494	0.527
L3	0.971	0.486	0.542
L4	0.986	0.518	0.548
L5	1.000	0.576	0.557
L6	0.982	0.571	0.554
L7	0.943	0.542	0.549

A comparison between measured data and the obtained 3-parameter Weibull CDF for L5 is shown in Figure 8. It should be noted that Weibull CDF cannot be fitted for H_S classes which have mean value of class (\bar{H}_S) lower than ε . Thus, Weibull CDF was not fitted to the lowest H_S class, which has a \bar{H}_S of 0.25 m. As shown in Figure 8, the 3-parameter Weibull CDF credibly describes measured data, and therefore, can be used for extreme value analyses. The obtained extreme values of H_S at the investigated locations are shown in Table 6.

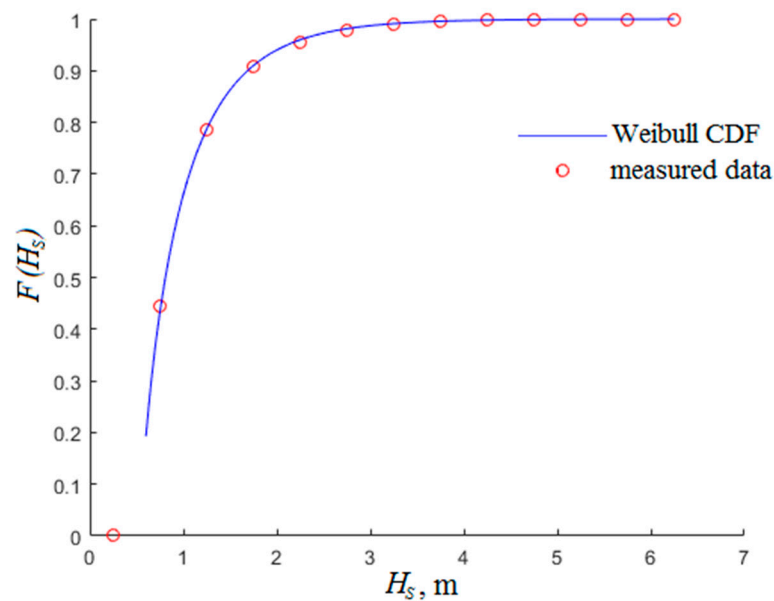


Figure 8. Comparison between measured data and the 3-parameter Weibull CDF.

Table 6. The obtained extreme values of H_S .

Location/RP	$H_S^{RP=1}$, m	$H_S^{RP=5}$, m	$H_S^{RP=10}$, m	$H_S^{RP=20}$, m	$H_S^{RP=50}$, m	$H_S^{RP=100}$, m	$H_{S,meas,max}$, m
L1	4.493	5.445	5.860	6.277	6.832	7.254	6.190
L2	4.660	5.643	6.071	6.500	7.072	7.506	6.720
L3	4.298	5.154	5.525	5.896	6.388	6.761	5.890
L4	4.434	5.306	5.682	6.058	6.557	6.934	5.170
L5	4.758	5.687	6.087	6.486	7.015	7.415	6.050
L6	4.867	5.839	6.258	6.678	7.234	7.656	6.330
L7	5.003	6.053	6.509	6.967	7.575	8.038	6.220

The obtained extreme values for $RP = 20$ years were compared with the measured data. Namely, since waves were measured for 23.5 years, the maximum value of H_S ($H_{S,meas,max}$) at certain location is shown in Table 6 as well. As shown in Table 6, the obtained extreme values of H_S show satisfactory agreement with the measured values. However, for a more reliable comparison, the obtained extreme values should be compared with in situ measurements using buoys at those locations. Based on the obtained extreme values, it can be concluded that the most severe conditions occurred at L7, with a $H_S^{RP=100}$ of 8.038 m. Even though L4 has the most favourable wave energy potential, the obtained extreme values at this location were second lowest of all the investigated locations. Thus, the obtained $H_S^{RP=100}$ at L4 was 6.934 m, while the $H_S^{RP=50}$ was 6.557 m. Therefore, considering that WECs are usually designed for the return period of 20 to 40 years, the potential infrastructure costs in terms of the structural reliability could be lower [30].

3.2. Offshore Wind Energy Potential

In order to investigate the feasibility of harvesting wave energy in the Croatian part of the Adriatic Sea, the offshore wind energy potential was assessed. The obtained results are presented in Table 7.

Table 7. Offshore wind energy potential.

Location	P_{EW} , GWh	$P_{EW,average}$, kW
L1	3.256	371.640
L2	2.946	336.271
L3	3.586	409.406
L4	2.656	303.220
L5	2.656	303.220
L6	2.946	336.271
L7	3.586	409.406

As shown in Table 7, the annual wind energy is one order of magnitude larger than the annual wave energy in the Croatian part of the Adriatic Sea. Furthermore, the cost of offshore wind energy per MWh is lower than the cost of offshore wave energy per MWh [42]. Thus, it can be concluded that at present, wave harvesting in the Croatian part of the Adriatic Sea is not economically justifiable. One of the reasons for this can be attributed to the limited fetch length which prevents full development of the sea. Thus, even though the strong winds over the Adriatic Sea can reach storm conditions, the sea will not develop fully as it would in non-limited fetch areas. Therefore, waves have lower energy, i.e., lower wave energy periods. Namely, the mean annual values of T_E at the investigated locations are in the range from 3.5 to 4.2 s. For example, the mean annual T_E along the shore of Santa Catarina in Brazil, where the fetch length is not limited [13], is approximately 9.5 s. This leads to significantly higher wave energy potential. Also, since the Adriatic Sea is a semi-enclosed sea, swells are quite low. For that reason, the wave height is mainly due to wind, and as mentioned, due to limited fetch, the sea cannot be fully developed.

4. Conclusions

The offshore wave energy potential was assessed at seven locations in the Croatian part of the Adriatic Sea utilising satellite measurement data. This data was used for the creation of wave roses, wave power diagrams and for the characterisation of the yearly energy. The mean yearly wave energy was calculated for two offshore WECs, i.e., Aqua Buoy and Pelamis. Furthermore, an extreme value analysis was performed utilising statistical analyses of waves. Among the investigated locations, L4 appeared to be the best for wave harvesting, even though the highest mean wave power was obtained at location L6. This is attributed to the more energetic sea states at location L4 compared to L6. What is more, the extreme value analysis showed that L4 had second lowest extreme values of H_S , which is important for structural reliability. The bulk of the wave power at locations L3, L5, L6 and L7 comes from south-easterly waves, at locations L1 and L2 from north-easterly waves, and at location L4 from northerly, south-easterly and southerly waves. Seasonal variability of the wave power at all locations is highlighted with the highest wave power present in the winter, and only slightly lower wave power present in the autumn. However, in the spring, wave power is less than half that of the winter, and in the summer, it is even lower. The mean yearly wave energy for Aqua Buoy at L4 was approximately 50 MWh, while that of Pelamis was approximately 230 MWh. Locations L5, L6 and L7 had a P_E of around 37 MWh for Aqua Buoy and around 200 MWh for Pelamis. Locations L1, L2 and L3 had a significantly lower P_E : for Aqua Buoy below 20.5 MWh and for Pelamis below 125 MWh. In order to evaluate the WEC performance, capacity factors were estimated for annual and seasonal levels. Low capacity factors were obtained for both the investigated WECs, and the higher capacity factors were obtained for Pelamis. Significant variation regarding seasonal performance was noticed, e.g., the autumn and winter capacity factors were higher than in the spring and summer. It should be noted that within this study, Aqua buoy, which has diameter of 6 m and a draught of 30 m, as well as Pelamis, which has a length of 150 m and a diameter of 4.63 m, were investigated. Since low capacity factors were obtained, it would be beneficial to investigate the performance of smaller rated devices at the investigated locations. Thus, the investigated WECs should be down-scaled, and the associated power

matrix could be determined using Froude similarity, which is commonly done in physical modellings of WECs [29]. Down-scaled WECs would have higher capacity factors, as their idle period would be reduced, and therefore more suitable and favorable for the application. Smaller WECs could produce electricity at lower sea states, which are dominant in the Croatian part of the Adriatic Sea. Therefore, the investigation of the application of smaller WECs in the Croatian part of the Adriatic Sea and the determination of the optimum scale for these locations will form the basis for future work.

The obtained P_E at the investigated locations were compared with the mean yearly wind energy; it was shown that wind energy is one order of magnitude higher than wave energy. This was attributed to the strong winds present in the Adriatic Sea, which, due to limited fetch, cannot fully develop in the sea. Also, since the Adriatic Sea is a semi-enclosed sea, swells are quite low. Therefore, waves in the Croatian part of the Adriatic Sea have small wave energy periods. It should be noted that wave energy harvesting is still at the early stages of development, and therefore, a potential solution for the acceleration of its development is the combination of two different energy resources. Thus, wind-wave farming could compensate for wind variability and allow continuous energy harvesting to occur.

Author Contributions: The research team works in a collaborative manner and all the authors have contributed in all the sections of the present manuscript.

Funding: This research received no external funding.

Acknowledgments: This study has been supported by the Croatian Science Foundation under project 8658. The WorldWaves data used in the paper is supplied by Fugro OCEANOR AS.

Conflicts of Interest: The authors declare no conflict of interest.

Appendix A

Table A1. WWA wave and wind parameters.

Significant wave height	H_S, m
Mean wave direction	$\vartheta, ^\circ$
Peak period of 1D spectra	T_P, s
Mean wave period/Energy period	T_E, s
Significant wave height of wind waves	H_{SW}, m
Mean direction of wind waves	$\vartheta_W, ^\circ$
Mean period of wind waves	T_{EW}, s
Significant wave height of primary swell	H_{SS}, m
Mean direction of primary swell	$\vartheta_S, ^\circ$
Mean period of primary swell	T_{ES}, s
Wind speed at 10 m height	$v_{W10}, m/s$
Wind direction at 10 m height	$\vartheta_{W10}, ^\circ$

Table A2. Power matrix for WEC Aqua Buoy [31].

$H_S(m)/T_E(s)$	5.5	6.5	7.5	8.5	9.5	10.5	11.5	12.5	13.5	14.5	15.5	16.5
0.75	0	8	11	12	11	10	8	7	0	0	0	0
1.25	13	17	25	27	26	23	19	15	12	12	12	7
1.75	24	30	44	49	47	41	34	28	23	23	23	12
2.25	37	47	69	77	73	64	54	43	36	36	36	19
2.75	54	68	99	111	106	92	77	63	51	51	51	27
3.25	0	93	135	152	144	126	105	86	70	70	70	38
3.75	0	0	122	176	198	188	164	137	112	91	91	49
4.25	0	0	223	250	239	208	173	142	115	115	115	62
4.75	0	0	250	250	250	250	214	175	142	142	142	77
5.25	0	0	250	250	250	250	250	211	172	172	172	92

Table A3. Power matrix for WEC Pelamis [31].

$H_S(m)/T_E(s)$	4.75	5.25	5.75	6.25	6.75	7.25	7.75	8.25	8.75	9.25	9.75	10.25	10.75	11.25	11.75	12.25	12.75
0.75	0	22	29	34	37	38	38	37	35	32	29	26	23	21	0	0	0
1.25	32	50	65	76	83	86	86	83	78	72	65	59	53	47	42	37	33
1.75	57	88	115	136	148	153	152	147	138	127	116	104	93	83	74	66	59
2.25	89	138	180	212	231	238	238	230	216	199	181	163	146	130	116	103	92
2.75	129	198	260	305	332	340	332	315	292	266	240	219	210	188	167	149	132
3.25	0	270	354	415	438	440	424	404	377	362	326	292	260	230	215	202	180
3.75	0	0	462	502	540	546	530	499	475	429	384	366	339	301	267	237	213
4.25	0	0	544	635	642	648	628	590	562	528	473	432	382	356	338	300	266
4.75	0	0	0	739	726	731	707	687	670	607	557	521	472	417	369	348	328
5.25	0	0	0	750	750	750	750	750	737	667	658	586	530	496	446	395	355
5.75	0	0	0	0	750	750	750	750	750	750	711	633	619	558	512	470	415
6.25	0	0	0	0	750	750	750	750	750	750	750	743	658	621	579	512	481
6.75	0	0	0	0	0	750	750	750	750	750	750	750	750	676	613	584	525
7.25	0	0	0	0	0	0	750	750	750	750	750	750	750	750	686	622	593
7.75	0	0	0	0	0	0	0	750	750	750	750	750	750	750	750	690	625

References

1. Leeney, R.H.; Greaves, D.; Conley, D.; O'Hagan, A.M. Environmental Impact Assessments for wave energy developments—Learning from existing activities and informing future research priorities. *Ocean Coast. Manag.* **2014**, *99*, 14–22. [[CrossRef](#)]
2. Monteforte, M.; Re, C.L.; Ferreri, G.B. Wave energy assessment in Sicily (Italy). *Renew. Energy* **2015**, *78*, 276–287. [[CrossRef](#)]
3. Lehmann, M.; Karimpour, F.; Goudey, C.A.; Jacobson, P.T.; Alam, M.R. Ocean wave energy in the United States: Current status and future perspectives. *Renew. Sustain. Energy Rev.* **2017**, *74*, 1300–1313. [[CrossRef](#)]
4. Komporn, W.; Ekkawatpanit, C.; Kositgittiwong, D. Assessment of ocean wave energy resource potential in Thailand. *Ocean Coast. Manag.* **2018**, *160*, 64–74. [[CrossRef](#)]
5. Liang, B.; Shao, Z.; Wu, G.; Shao, M.; Sun, J. New equations of wave energy assessment accounting for the water depth. *Appl. Energy* **2017**, *188*, 130–139. [[CrossRef](#)]
6. Franzitta, V.; Curto, D. Sustainability of the renewable energy extraction close to the Mediterranean Islands. *Energies* **2017**, *10*, 283. [[CrossRef](#)]
7. Bento, A.R.; Martinho, P.; Soares, C.G. Wave energy assessment for Northern Spain from a 33-year hindcast. *Renew. Energy* **2018**, *127*, 322–333. [[CrossRef](#)]
8. Hemer, M.A.; Zieger, S.; Durrant, T.; O'Grady, J.; Hoeke, R.K.; McInnes, K.L.; Rosebrock, U. A revised assessment of Australia's national wave energy resource. *Renew. Energy* **2017**, *114*, 85–107. [[CrossRef](#)]
9. López, M.; Veigas, M.; Iglesias, G. On the wave energy resource of Peru. *Energy Convers. Manag.* **2015**, *90*, 34–40. [[CrossRef](#)]
10. Aboobacker, V.M. Wave energy resource assessment for eastern Bay of Bengal and Malacca Strait. *Renew. Energy* **2017**, *114*, 72–84. [[CrossRef](#)]
11. Quitaras, M.R.D.; Abundo, M.L.S.; Danao, L.A.M. A techno-economic assessment of wave energy resources in the Philippines. *Renew. Sustain. Energy Rev.* **2018**, *88*, 68–81. [[CrossRef](#)]
12. Lucero, F.; Catalán, P.A.; Ossandón, Á.; Beyá, J.; Puelma, A.; Zamorano, L. Wave energy assessment in the central-south coast of Chile. *Renew. Energy* **2017**, *114*, 120–131. [[CrossRef](#)]
13. Contestabile, P.; Ferrante, V.; Vicinanza, D. Wave energy resource along the coast of Santa Catarina (Brazil). *Energies* **2015**, *8*, 14219–14243. [[CrossRef](#)]
14. Sierra, J.P.; Martín, C.; Mösso, C.; Mestres, M.; Jebbad, R. Wave energy potential along the Atlantic coast of Morocco. *Renew. Energy* **2016**, *96*, 20–32. [[CrossRef](#)]
15. Bernardino, M.; Rusu, L.; Soares, C.G. Evaluation of the wave energy resources in the Cape Verde Islands. *Renew. Energy* **2017**, *101*, 316–326. [[CrossRef](#)]
16. Aboobacker, V.M.; Shanass, P.R.; Alsaafani, M.A.; Albarakati, A.M. Wave energy resource assessment for Red Sea. *Renew. Energy* **2017**, *114*, 46–58. [[CrossRef](#)]
17. Alamian, R.; Shafaghat, R.; Hosseini, S.S.; Zainali, A. Wave energy potential along the southern coast of the Caspian Sea. *Int. J. Mar. Energy* **2017**, *19*, 221–234. [[CrossRef](#)]

18. Wang, Z.; Dong, S.; Dong, X.; Zhang, X. Assessment of wind energy and wave energy resources in Weifang sea area. *Int. J. Hydrogen Energy* **2016**, *41*, 15805–15811. [[CrossRef](#)]
19. Kamranzad, B.; Etemad-Shahidi, A.; Chegini, V. Developing an optimum hotspot identifier for wave energy extracting in the northern Persian Gulf. *Renew. Energy* **2017**, *114*, 59–71. [[CrossRef](#)]
20. Wang, Z.; Dong, S.; Li, X.; Soares, C.G. Assessments of wave energy in the Bohai Sea, China. *Renew. Energy* **2016**, *90*, 145–156. [[CrossRef](#)]
21. Mørk, G.; Barstow, S.; Kabuth, A.; Pontes, M.T. Assessing the global wave energy potential. In Proceedings of the 29th International Conference on Ocean, Offshore and Arctic Engineering, Shanghai, China, 6–11 June 2010; p. 20473.
22. Arena, F.; Laface, V.; Malara, G.; Romolo, A.; Viviano, A.; Fiamma, V.; Sannino, G.; Carillo, A. Wave climate analysis for the design of wave energy harvesters in the Mediterranean Sea. *Renew. Energy* **2015**, *77*, 125–141. [[CrossRef](#)]
23. Besio, G.; Mentaschi, L.; Mazzino, A. Wave energy resource assessment in the Mediterranean Sea on the basis of a 35-year hindcast. *Energy* **2016**, *94*, 50–63. [[CrossRef](#)]
24. Vannucchi, V.; Cappietti, L. Wave energy assessment and performance estimation of state of the art wave energy converters in Italian hotspots. *Sustainability* **2016**, *8*, 1300. [[CrossRef](#)]
25. Liberti, L.; Carillo, A.; Sannino, G. Wave energy resource assessment in the Mediterranean, the Italian perspective. *Renew. Energy* **2013**, *50*, 938–949. [[CrossRef](#)]
26. Franzitta, V.; Curto, D.; Milone, D.; Rao, D. Assessment of renewable sources for the energy consumption in Malta in the Mediterranean Sea. *Energies* **2016**, *9*, 1034. [[CrossRef](#)]
27. Lavidas, G.; Venugopal, V. Wave energy resource evaluation and characterisation for the Libyan Sea. *Int. J. Mar. Energy* **2017**, *18*, 1–14. [[CrossRef](#)]
28. Vicinanza, D.; Cappietti, L.; Contestabile, P. Assessment of wave energy around Italy. In Proceedings of the 8th European Wave and Tidal Energy Conference, Uppsala, Sweden, 7–10 September 2009; pp. 256–262.
29. Bozzi, S.; Archetti, R.; Passoni, G. Wave electricity production in Italian offshore: A preliminary investigation. *Renew. Energy* **2014**, *62*, 407–416. [[CrossRef](#)]
30. Lavidas, G.; Venugopal, V. Energy Production Benefits by Wind and Wave Energies for the Autonomous System of Crete. *Energies* **2018**, *11*, 2741. [[CrossRef](#)]
31. Silva, D.; Rusu, E.; Soares, C.G. Evaluation of various technologies for wave energy conversion in the Portuguese nearshore. *Energies* **2013**, *6*, 1344–1364. [[CrossRef](#)]
32. Rusu, E. Evaluation of the wave energy conversion efficiency in various coastal environments. *Energies* **2014**, *7*, 4002–4018. [[CrossRef](#)]
33. Barstow, S.; Mork, G.; Lonseth, L.; Schjolberg, P.; Machado, U.; Athanassoulis, G.; Belibassakis, K.; Gerostathis, T.; Stefanakos, C.; Spaan, G. WORLDWAVES: Fusion of data from many sources in a user-friendly software package for timely calculation of wave statistics in global coastal waters. In Proceedings of the 13th International Offshore and Polar Conference and Exhibition, ISOPE2003, Honolulu, HI, USA, 25–30 May 2003; pp. 136–143.
34. Katalinić, M.; Parunov, J. Wave statistics in the Adriatic Sea based on 24 years of satellite measurements. *Ocean Eng.* **2018**, *158*, 378–388. [[CrossRef](#)]
35. Analysis of Cost Reduction Opportunities in the Wave Energy Industry. Available online: http://www.esru.strath.ac.uk/EandE/Web_sites/14-15/Wave_Energy/point-absorber.html (accessed on 16 May 2019).
36. Guillou, N.; Chapalain, G. Annual and seasonal variabilities in the performances of wave energy converters. *Energy* **2018**, *165*, 812–823. [[CrossRef](#)]
37. Li, W.; Isberg, J.; Waters, R.; Engström, J.; Svensson, O.; Leijon, M. Statistical analysis of wave climate data using mixed distributions and extreme wave prediction. *Energies* **2016**, *9*, 396. [[CrossRef](#)]
38. Farkas, A.; Parunov, J.; Katalinic, M. Wave statistics for the middle Adriatic Sea. *J. Marit. Transp. Sci.* **2016**, *52*, 33–47. [[CrossRef](#)]
39. Hadžić, N.; Kozmar, H.; Tomić, M. Offshore renewable energy in the Adriatic Sea with respect to the Croatian 2020 energy strategy. *Renew. Sustain. Energy Rev.* **2014**, *40*, 597–607. [[CrossRef](#)]
40. Državni Hidrometeorološki Zavod. Available online: www.meteo.hr (accessed on 16 May 2019).
41. NWE Sales, Windmill Sales and Engineering. Available online: <http://www.nwesales.fi/windpower/> (accessed on 29 May 2019).

42. Astariz, S.; Iglesias, G. The economics of wave energy: A review. *Renew. Sustain. Energy Rev.* **2015**, *45*, 397–408. [[CrossRef](#)]



© 2019 by the authors. Licensee MDPI, Basel, Switzerland. This article is an open access article distributed under the terms and conditions of the Creative Commons Attribution (CC BY) license (<http://creativecommons.org/licenses/by/4.0/>).